

Restrictions on shareability of classical correlations for random multipartite quantum states

Saptarshi Roy, Shiladitya Mal, and Aditi Sen(De) *Harish-Chandra Research Institute and HBNI, Chhatnag Road, Jhansi, Allahabad-211019, India* (Received 23 September 2020; revised 27 February 2021; accepted 31 March 2021; published 3 May 2021)

Unlike quantum correlations, the shareability of classical correlations (CCs) between two parties of a multipartite state is assumed to be free since there exist states for which CCs for each of the reduced states can simultaneously reach their algebraic maximum value. However, when one randomly picks out states from the state space, we find that the probability of obtaining those states possessing the algebraic maximum value is vanishingly small. Therefore, the possibility of a nontrivial upper bound on the distribution of CCs that is less than the algebraic maxima emerges. We explore this possibility by Haar uniformly generating random multipartite states and computing the frequency distribution for various CC measures, conventional classical correlators, and two axiomatic measures of classical correlations, namely, the classical part of quantum discord and local work of work-deficit. We find that the distributions are typically Gaussian-like and their standard deviations decrease with the increase in number of parties. It also reveals that, among the multiqubit random states, most of the reduced density matrices possess a low amount of CCs which can also be confirmed by the mean of the distributions, thereby showing a kind of restrictions on the shareability of classical correlations for random states. Furthermore, we also notice that the maximal value for random states is much lower than the algebraic maxima obtained for a set of states, and the gap between the two increases further for states with a higher number of parties. We report that, for a higher number of parties, the classical part of quantum discord and local work can follow a monogamy-based upper bound on shareability while classical correlators have a different upper bound. The trends of shareability for classical correlation measures in random states clearly demarcate between the axiomatic definition of classical correlations and the conventional ones.

DOI: [10.1103/PhysRevA.103.052401](https://doi.org/10.1103/PhysRevA.103.052401)

I. INTRODUCTION

In a multipartite system, the rule according to which a certain physical property is shared among different subsystems is assigned by a specific theory. In particular, for a given theory which can be quantum mechanics [1] or generalized probabilistic theory [2], the physical characteristics, say, \mathcal{P} , of reduced states of a multipartite state, $\rho_{1\dots N}$ shared by N parties situated at different locations can be upper bounded by a fixed value, thereby establishing the restrictions on shareability of that physical component. The mathematical formulation of it reads

$$\sum_{i=2}^N \mathcal{P}(\rho_{1i}) \leq U, \quad (1)$$

where ρ_{1i} is the reduced state of $\rho_{1\dots N}$ and U is an upper bound of the shareability condition. Like no-go theorems for single quantum systems [3–8], constraints proved on sharing of properties like entanglement, violation of Bell inequalities, capacities of dense coding and teleportation in a multipartite quantum system [9–22] play an important role in quantum information processing tasks.

The unbounded sharing of quantum correlations among a pair of parties in a multipartite state is forbidden—a concept known as monogamy of quantum correlations (QCs) [9,23]. In particular, if two of the parties of a multipartite state share maximal QC, they cannot share any QC with other parties. Monogamy of QC also has an impact on several quantum

information processing tasks which include quantum cryptography and entanglement sharing in a quantum network [24–26]. In a seminal paper by Coffman, Kundu, and Wootters [9], such a qualitative concept of monogamy got a mathematical form that can be used to check whether a QC measure follows a monogamy inequality. Specifically, a QC measure, \mathcal{Q} , is said to follow a monogamy relation [27,28] if

$$\delta_{\mathcal{Q}} = \mathcal{Q}_{1:2\dots N} - \sum_{i=2}^N \mathcal{Q}_{1i} \geq 0, \quad (2)$$

where $\mathcal{Q}_{1:2\dots N} \equiv \mathcal{Q}(\rho_{1:2\dots N})$, $\mathcal{Q}_{1i} \equiv \mathcal{Q}(\rho_{1i})$, $i = 2, \dots, N$, of a multipartite state $\rho_{12\dots N}$ and $\delta_{\mathcal{Q}}$ can be referred as QC monogamy score [27]. In other words, although each term in $\sum_{i=2}^N \mathcal{Q}_{1i}$ can reach $\log_2 d$ (excepting measures like negativity and logarithmic negativity [29]) in a N -qudit system, sharing of QC is bounded above only by a quantum correlation content in the 1 : rest-bipartition. Note that the party, 1, has a special status and can be referred to as a nodal observer. Similar to such inequality can also be derived with other parties as nodal observer. It is known that monogamy scores of squared concurrence [9,30], negativity [29,31,32], and quantum discord [20,33–37] are non-negative. Moreover, it was shown that all QC measures for random multipartite quantum states tend to become monogamous when the number of parties increases [38–41].

In stark contrast, classical correlations (CCs) do not possess such restrictions. Specifically, there exists a multipartite

state for which any CC quantifier between reduced two-party states can simultaneously reach its maximal value and hence the upper bound in Eq. (1) scales with the increase in the number of parties. However, it should be noted that, unlike QC measure, it is not yet settled when a quantity can measure reliably the amount of CC present even in a bipartite quantum state. Over the years, a few measures of CC were proposed—prominent ones having diverse origins include CC part in quantum discord (CQD) [33–35], extractable local work (LW) [42], and a conventional classical correlator (CCC), defined as $\text{tr}(\sigma^k \otimes \sigma^l \rho_{12})$ for a bipartite state, ρ_{12} which have been used in quantum mechanics, ranging from Bell inequalities [43,44] to many-body physics [45]. CQD and LW are defined operationally and satisfy some axioms which a bona fide measure of CC is supposed to obey.

In this paper, we address the following questions:

(1) Can we obtain a nontrivial upper bound [U in Eq. (1)] on the shareability of CC among bipartite reduced states of random multipartite systems?

(2) Second, how does the frequency distribution, and consequently the bound for sharing of CC among bipartite reduced states obtained from random multipartite states, change with the increase in system size?

We report here that the answer to the first question is affirmative, and hence a new rule for the shareability of CC among subsystems emerges for random multipartite states. Investigating on Haar uniformly generated random multipartite states [46], we find several counterintuitive results. For systematic analysis, the shareability for classical correlations is addressed from two perspectives, which we refer to as “unconstrained” and “constrained” settings. The constrained one implies that the sample of random states that we choose for our analysis possesses a fixed, or a definite range of values of a particular physical property (classical or quantum) different from the one under investigation while the unconstrained one does not have such restrictions. By carrying out our investigations for $N = 3$ to 6 multiqubit random pure states, we observe that, like QC, maximal shareability of CC is also restricted, rather the algebraic maximum occurs only for sets of states with vanishingly small measure. In the case of an unconstrained scenario, the frequency distributions of the shareability constraints for random states [i.e., the left-hand side in Eq. (1)] take the form of a Gaussian, irrespective of the choices of the CC measures, and the Gaussian-like shapes become narrower for a greater number of qubits, thereby showing the decrease in standard deviation with the increase of number of parties. On the other hand, the mean value of CCC remains almost constant over increasing system size, while the means of CQD and LW decrease. Moreover, their maximum values obtained via numerical simulations decrease with the increase in the number of parties. We also find a kind of trade-off for maximal values of CCCs in complementary directions.

In the case of a constrained framework, we consider two kinds of constraints—for a definite value of CCC in a fixed direction, we study the behavior of sharing rule for CCC in complementary direction and we also investigate the consequence on average as well as the maximum value of $\sum_{i=2}^N \mathcal{P}_{1i}$ for the CC measures when randomly generated states possess a definite range of genuine multipartite entanglement.

Interestingly, we notice that, with the increase of genuine multipartite entanglement, the average value for the shareability of CQD and LW in the subsystems of random multipartite states diminishes. Such an observation leads to the result that LW and CQD follow the monogamy-based upper bound with a very high percentage of random states having a higher number of parties which CCC fails to satisfy.

The paper is organized in the following way: In Sec. II, we discuss the classical correlation measures, and the class of states for which shareability of CC measures reach their maximum value. Section III deals with the patterns in the distribution of CC in multiqubit random states while we discuss how the sharing properties of CC changes when a fixed amount of other CC measure or a genuine multipartite entanglement measure is present in random states in Sec. IV. We check whether the monogamy-motivated upper bound on shareability of CC measures is good in Sec. V, and conclude in Sec. VI.

II. CLASSICAL CORRELATION MEASURES AND THEIR ALGEBRAIC MAXIMA

Let us describe briefly three types of classical correlation (CC) measures and their properties for an arbitrary bipartite shared state ρ_{12} . Unlike entanglement measures [47], the properties that a “good” classical correlation measure of quantum states should follow are not well understood. However, there are CC measures introduced in Refs. [33–35] which follow the following properties: (1) it should be vanishing for $\rho_1 \otimes \rho_2$, (2) it is invariant under local unitary transformations, (3) it should be nonincreasing under local operations, and (4) it reduces to $S(\rho_1) = S(\rho_2)$ for pure bipartite states $|\psi\rangle_{12}$ with ρ_1 and ρ_2 being the corresponding local density matrices. We will also consider another CC measure introduced from the perspective of thermodynamics and the conventional classical correlators, appearing in the definition of density matrices [43], which play an important role in different fields ranging from Bell inequalities [44] to many-body physics [45] (see also Refs. [48,49]).

We first give the definitions of two classical correlation measures [35] associated with quantum discord (QD) and one-way work-deficit where the former do follow the postulates of CC measure while the latter satisfies the first two and the third one with modifications. We refer to both these CC measures as axiomatic measures. The classical correlation part of quantum discord (CQD) of ρ_{12} can be defined as

$$C^D(\rho_{12}) \equiv C_{12}^D = S(\rho_1) - \min_{\{P_i\}} \sum_i p_i S(\rho_{1|i}), \quad (3)$$

where $S(\rho) = -\text{tr}(\rho \log_2 \rho)$ is the von Neumann entropy,

$$\rho_{1|i} = \frac{\text{tr}_2(I \otimes P_i \rho_{12} I \otimes P_i)}{\text{tr}(I \otimes P_i \rho_{12} I \otimes P_i)}, \quad (4)$$

with P_i being the rank-1 projective measurements on the second party and $p_i = \text{tr}(I \otimes P_i \rho_{12} I \otimes P_i)$. Here the minimization is performed over all rank-1 projective measurements. A similar definition emerges when the measurement is done on the first party. Notice that, in the definition of QD, the optimization is taken over the most general measurements, i.e., positive operator valued measurements (POVMs).

However, it was shown via numerical simulations that projective measurements yield very close to the optimal value obtained via POVMs. So from the practical viewpoint of computational simplicity, we perform our analysis with projective measurements.

Motivated by quantum thermodynamics, the classical correlation can also be quantified as local extractable work (LW) by closed local operations and one-way classical communication [35,42] consisting of local unitaries, local dephasings, and sending dephased states from one party to another. Mathematically, LW reads

$$\tilde{C}^{\text{LW}}(\rho_{12}) \equiv \tilde{C}_{12}^{\text{LW}} = \log_2 d_{12} - \min_{\{P_i\}} S\left(\sum_i p_i \rho_{1i}\right), \quad (5)$$

where p_i and ρ_{1i} are same as in Eq. (4), and $d_{12} = d_1 d_2$ is the dimension of ρ_{12} with the individual subsystems having dimensions, d_1 and d_2 . Note that \tilde{C}^{LW} can take values up to $\log_2 d_{12}$ and to make it consistent with other measures of classical correlation, which take values from 0 to 1, we scale \tilde{C}^{LW} with $\log_2 d_{12}$ and call it $C^{\text{LW}} = \frac{1}{\log_2 d_{12}} \tilde{C}^{\text{LW}}$.

Let us now define conventional two-site classical correlator present in any two-qubit state, given by

$$\rho_{12} = \frac{1}{4} \left[I \otimes I + \sum_{k=x,y,z} (m^k \sigma^k \otimes I + m^k I \otimes \sigma^k) + \sum_{k,l=x,y,z} C^{kl} \sigma^k \otimes \sigma^l \right]. \quad (6)$$

Here

$$C^{kl} = \text{tr}(\sigma^k \otimes \sigma^l \rho_{12}), \quad k, l = x, y, z. \quad (7)$$

represents the two-site classical correlators which leads to the correlation matrix having diagonal elements C^{kk} , $k = x, y, z$ and off-diagonal ones, C^{kl} , $k \neq l$. $m^k = \text{tr}(\sigma^k \rho_1)$, $m^k = \text{tr}(\sigma^k \rho_2)$, $k = x, y, z$ denote the magnetizations corresponding to the single site density matrix of ρ_{12} . Note that C^{kl} does not follow the properties mentioned above and hence we may expect to see different universal behavior for random states than that of C^D and \tilde{C}^{LW} . Since the classical correlators varies from -1 to 1 , we scale its range from 0 to 1 , by taking the absolute value of the same. Since from now on, we will always use the absolute values of these correlators, we drop the absolute bars, and any reference to C_{1i}^{kl} means the absolute value of the quantity, unless mentioned otherwise.

As stated earlier, we aim to investigate the pattern in the distributions of $\sum_{i=2}^N C_{1i}^D$, $\sum_{i=2}^N C_{1i}^{\text{LW}}$, and $\sum_{i=2}^N C_{1i}^{kl}$, as well as their nontrivial upper bounds for random multipartite states, $\rho_{12\dots N}$ by varying the number of parties. We are also interested to compute the corresponding statistical quantities like different moments of the distributions and compare them. Unlike QCs, we first notice that each quantity in the sum can simultaneously take the maximum value, unity for qubits. In the next section, we identify classes of multipartite states for which the algebraic maxima of CC measures can be obtained. However, we want to study whether the algebraic maximum value of these quantities can also be reached for randomly generated states.

A. Class of states maximizing classical correlation measures

Before continuing our study with random states, let us determine the class of states for which all individual two-party classical correlations in a multiqubit state simultaneously reach algebraically maximal values. Specifically, we identify states which maximize $\sum_{i=2}^N C_{1i}$. For two-qubit states, since each C_{1i} can be unity, $\sum_{i=2}^N C_{1i}$ can, in principle, reach $N - 1$. For all the CC measures discussed above, it is indeed possible to saturate that bound for a certain types of states. To illustrate this, we consider product states, $|0\rangle^{\otimes N}$ and $|1\rangle^{\otimes N}$ as well as the Greenberger-Horne-Zeilinger (GHZ) state [50] $|GHZ\rangle = \frac{1}{\sqrt{2}}(|0\rangle^{\otimes N} + |1\rangle^{\otimes N})$, which also possesses the maximal amount of genuine multiparty entanglement [51]. Note that, for the GHZ state, all bipartite reduced states with party 1 as the nodal observer read as $\rho_{1i} = \frac{1}{2}|00\rangle\langle 00| + \frac{1}{2}|11\rangle\langle 11|$, for $i \geq 2$, while all single-party reductions are the same which is the maximally mixed state, i.e., $\rho_j = \frac{1}{2}\mathbb{I}_2$ for all $j \in [1, N]$.

(1) *For the classical correlator(s)* $\tilde{C}_{1i}^{zz} = |\langle \sigma_z \otimes \sigma_z \rangle_{1i}| = |\text{tr}(\sigma_z \otimes \sigma_z \rho_{1i})| = 1$ for the $|GHZ\rangle$ state. Naturally, we also get the same results for the states $|0\rangle^{\otimes N}$ and $|1\rangle^{\otimes N}$. Thus, we have $\sum_{i=2}^N C_{1i}^{zz}$ is $N - 1$, the algebraic maximum for all three states. Let us now consider the covariance of C_{1i}^{zz} given by $\tilde{C}_{1i}^{zz} = |\langle \sigma_z \otimes \sigma_z \rangle_{1i} - \langle \sigma_z \rangle_1 \langle \sigma_z \rangle_i|$ for both $|0\rangle^{\otimes N}$ and $|1\rangle^{\otimes N}$. Now, $\langle \sigma_z \otimes \sigma_z \rangle_{1i} = \langle \sigma_z \rangle_1 \langle \sigma_z \rangle_i = 1$. Therefore, we get $\tilde{C}_{1i}^{zz} = 0$, identically. On the contrary, since for the GHZ state, $\langle \sigma_z \rangle_1 = \langle \sigma_z \rangle_i = \frac{1}{2} \text{tr}(\sigma_z I) = 0$, we obtain $\tilde{C}_{1i}^{zz}(|GHZ\rangle) = 1$. Hence, we have $\sum_{i=2}^N \tilde{C}_{1i}^{zz} = N - 1$ only for the GHZ state. Similar analysis can also be performed for other classical correlators and corresponding states can be identified.

(2) *Classical part of QD (CQD)*. Let us compute CQD of ρ_{1i} for the $|GHZ\rangle$ state. When a measurement is performed on the second party (i.e., the i th party) in the $\{|0\rangle, |1\rangle\}$ basis, we get pure postmeasurement states $|0\rangle$ and $|1\rangle$ with equal probabilities. Hence the second term of Eq. (3) vanishes, thereby maximizing the total quantity. Furthermore, the first term of Eq. (3) is unity since, as pointed earlier, all single-party reduced density matrices are maximally mixed states. Therefore, $C_{1i}^D(|GHZ\rangle) = 1$, and consequently by summing over i , we get the algebraic maximal value.

(3) *Local work*. The second term in the definition of C_{12}^{LW} in Eq. (5) takes the minimum value of zero for any pure product state $|\psi\rangle_1 \otimes |\psi\rangle_2$. Therefore, for any N -qubit pure completely product states $\otimes_{k=1}^N |\psi\rangle_k$, $C_{1i}^{\text{LW}} = \frac{1}{2}(2 - 0) = 1$. Consequently, we get $\sum_{i=2}^N C_{1i}^{\text{LW}} = N - 1$.

Note that, although we can possibly provide additional examples that give the algebraic maximal values, we unfortunately cannot provide an exhaustive set of states with this property. We think this, in general, is a difficult problem. Furthermore, note that numerical analysis would not help since the probability of a randomly generated state to reach the algebraically maximal value is vanishingly small.

Remark. In the Hilbert-Schmidt representation of a two-qubit state, the Bloch coefficients C^{kl} , $k, l = x, y, z$, form the elements of the correlation matrix. Any one of the nine coefficients does not contain any ‘‘quantum’’ properties, since a separable state also can possess exactly the same value of the given Bloch coefficient. However, when one takes all Bloch coefficients, i.e., the entire correlation matrix, of course it has

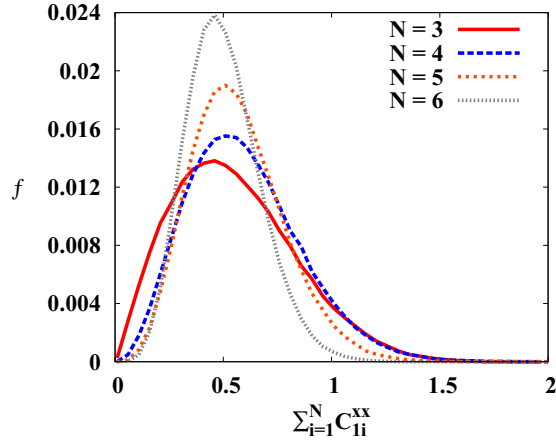


FIG. 1. Frequency distribution of $\sum_i C_{li}^{xx}$. The fraction f of states (vertical axis) is plotted against $\sum_i C_{li}^{xx}$ (horizontal axis) with a bin size of 0.01. Total number of random states generated for the analysis for each N is 10^6 . Note here that the covariance of $\sum_i C_{li}^{xx}$ also gives the similar frequency distribution, having almost the same mean and standard deviation. All the axes are dimensionless.

quantum properties and cannot be dubbed as merely classical. For example, the trace of the absolute values of the correlation matrix, $N = C^{xx} + C^{yy} + C^{zz}$, is directly connected to the average teleportation fidelity, $F = \frac{1}{2}(1 + N/3)$ [52]. Therefore, this by no means can be considered as classical. So, what we understood was that taking multiple Bloch coefficients simultaneously is tricky when we want to exclusively probe classical properties. So we resort to the use of single Bloch coefficients as a measure of classical correlation. As mentioned before, using covariances, we find that the classical correlation of $|00\rangle$ is zero ($\tilde{C}_{li}^{zz} = 0$). However, surprisingly, both variants of CC (single Bloch coefficients and the covariance-based ones) produced the same qualitative statistical features for Haar uniformly generated random states, as shown in Fig. 1. We present the results for the single Bloch coefficients for their wide applicability in various areas in quantum information science.

Notice that we keep these states out from our analysis since we are only concerned about properties of random multi-qubit states. When states are chosen randomly, the probability that one picks states from these classes is vanishingly small. Hence, a new upper bound lower than the algebraic maxima may emerge for almost all states (as sampled by Haar uniform generation [46]), since all the measure-zero states would naturally be eliminated from our analysis. The next section focuses on the possibility of any form of restriction on the distribution of classical correlations among bipartite reduced states of random multiparty quantum states.

III. TRENDS OF SHAREABILITY OF CLASSICAL CORRELATIONS FOR UNCONSTRAINED RANDOM STATES

We first generate three-, four-, five- and six-qubit pure states Haar uniformly [46] and compute their possible two-party reduced density matrices shared between the nodal observer and other parties, i.e., in our case, ρ_{li} , $i = 2, \dots, N$

TABLE I. Statistical data for the distribution of the fraction f of states obtained for $\sum_{i=2}^N C_{li}^{xx}$. The mean, standard deviation, and the maximum value of $\sum_{i=2}^N C_{li}^{xx}$ for randomly generated states are denoted respectively by ‘‘Mean,’’ ‘‘Sd,’’ and ‘‘Max val.’’ The total number of randomly generated state is 10^6 .

	N			
	3	4	5	6
Mean	0.546	0.589	0.559	0.497
Sd	0.281	0.258	0.214	0.170
Max val	1.856	2.101	2.026	1.441

obtained from a pure state, $|\psi\rangle_{12\dots N}$. From these generated states, we estimate sum of their CCs without imposing any additional condition on its properties and perform the analysis for the classical correlators, the classical part of quantum discord, and the local work of quantum work deficit.

A. Rule for distributing classical correlators in random multipartite states

We begin by looking at the CCCs, $C^{\alpha\beta}$, where $\alpha, \beta \in \{x, y, z\}$, as defined in Eq. (7). Our analysis reveals that all the $C^{\alpha\beta}$ display qualitatively and quantitatively similar features, and so without loss of generality, we focus on a particular one, say C^{xx} .

Let us enumerate below the observations of the distributions for $\sum_i C_{li}^{xx}$ as depicted in Fig. 1 and Table I:

(1) We trace out the fraction f of randomly generated states which possess $\sum C_{li}^{xx}$ values in a range denoted by a step size of 0.01 among 10^6 samples, i.e.,

$$f = \frac{\text{Number of states having values } \alpha < \sum C_{li}^{xx} \leq \alpha + 0.01}{\text{Total number generated states}},$$

where α is a fixed value of $\sum_i C_{li}^{xx}$, and 0.01 is the bin size in this case which will be changed depending on the analysis. We find that f depicts ‘‘Gaussian’’-like features for all chosen number of qubits, i.e., $N \leq 6$.

(2) *Mean and standard deviation.* With the increase of N , the standard deviation of the f distribution decreases, thereby making it more spiked, as shown in Fig. 1. However, mean of the distribution remains almost constant with N (see Table I).

(3) *Algebraic maximum.* For three-qubit random states, we can find states for which $\sum_{i=2}^3 C_{li}^{xx}$ is very close to its algebraic maximum, 2. However, for larger N values, the maximal value obtained for $\sum_{i=2}^N C_{li}^{xx}$ is much lower compared with the algebraic maximum $N - 1$, as can be seen also from the Table I.

Role of observable incompatibility

So far, all CCCs $C_{li}^{\alpha\beta}$ involved in the sum $\sum_{i=2}^N C_{li}^{\alpha\beta}$ have been the same, i.e., they possess the same α and β values for all $i \geq 2$. However, one may ask how the distribution changes if α and β change with i . In particular, it will be interesting to know how the distribution of f or the maximal value changes when the classical correlators for different i values do not commute.

For illustration, in the three-party case, we consider $C_{12}^{yx} + C_{13}^{xx}$. We find that, although the f distribution does not vary

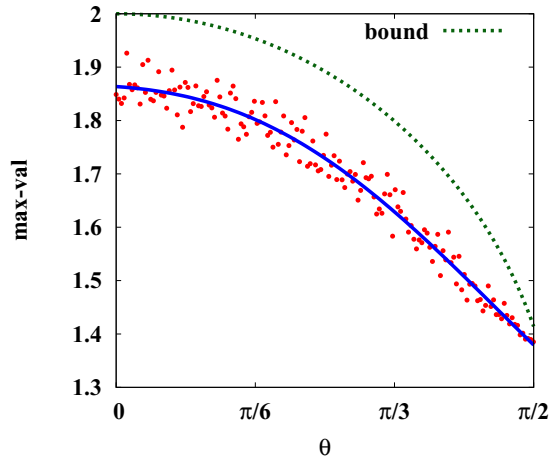


FIG. 2. Maximum of $C_{12}^{kx} + C_{13}^{kx}$ (y axis) vs θ (x axis) where k is the unit vector, $(\cos \theta, \sin \theta, 0)$. Red points represent maximal values of $C_{12}^{kx} + C_{13}^{kx}$ for different θ and the blue line is the best fit, depicting the decreasing nature with the increase of noncommutativity as measured by θ . Dotted line is the upper bound obtained in Eq. (14). All the axes are dimensionless.

much from $C_{12}^{xx} + C_{13}^{xx}$, the maximal value of the sum of the correlators decreases as operators become more incompatible in the sense of noncommutativity.

Toward checking it, we now investigate how the maximal value varies upon changing the commutativity of the operators, i.e., when the operators become noncommuting from the commuting ones. For a quantitative analysis, we compute the f distribution for $C_{12}^{kx} + C_{13}^{kx}$, where the direction k is defined by the unit vector $(\cos \theta, \sin \theta, 0)$. The corresponding local operator for the direction k is defined by $\cos \theta \sigma_x + \sin \theta \sigma_y$. Note that $\theta = 0$ represents the commuting case, while $\theta = \pi/2$ refers to the maximum noncommuting cases. As θ increases, i.e., when the amount of incompatibility between two operators increases, we observe that the maximal value of $C_{12}^{kx} + C_{13}^{kx}$ decreases, see Fig. 2. We now attempt to provide an upper bound of $C_{12}^{kx} + C_{13}^{kx}$, following the ideas in Refs. [18,53,54]. For this, we first consider two projectors A and B and construct an operator $M = A\langle A \rangle + B\langle B \rangle$. We now have the following:

$$\begin{aligned} \langle M \rangle &= \langle A \rangle^2 + \langle B \rangle^2, \\ \langle M^2 \rangle &= \langle M \rangle + \langle A \rangle \langle B \rangle \langle \{A, B\} \rangle, \end{aligned} \quad (8)$$

where $\{A, B\} = AB + BA$. Using the non-negativity of the variance $\langle M^2 \rangle - \langle M \rangle^2 \geq 0$ and approximating $\langle A \rangle \langle B \rangle = 1$, we arrive at the relation, given by

$$\langle M \rangle^2 - \langle M \rangle - \langle \{A, B\} \rangle \leq 0. \quad (9)$$

Since $\langle M \rangle \geq 0$, the above condition reduces to

$$\langle M \rangle \leq \frac{1}{2}(1 + \sqrt{1 + 4\langle \{A, B\} \rangle}). \quad (10)$$

Again, using the Cauchy-Schwarz inequality, we have

$$|\langle A \rangle| + |\langle B \rangle| \leq \sqrt{2}\sqrt{\langle A \rangle^2 + \langle B \rangle^2} = \sqrt{2}\sqrt{\langle M \rangle}. \quad (11)$$

Using Eq. (10), we finally obtain

$$|\langle A \rangle| + |\langle B \rangle| \leq 1 + \sqrt{1 + 4\langle \{A, B\} \rangle}. \quad (12)$$

If we now put $A = (\cos \theta \sigma_x + \sin \theta \sigma_y) \otimes \sigma_x \otimes \mathbb{I}_2$ and $B = \sigma_x \otimes \mathbb{I}_2 \otimes \sigma_x$, we get

$$\begin{aligned} \langle \{A, B\} \rangle &= 2 \cos \theta \langle \mathbb{I}_2 \otimes \sigma_x \otimes \sigma_x \rangle \\ &\quad + \sin \theta \langle (\{\sigma_x \otimes \sigma_y\}) \otimes \sigma_x \otimes \sigma_x \rangle \leq 2 \cos \theta. \end{aligned} \quad (13)$$

Furthermore, the above substitution makes $|\langle A \rangle| = C_{12}^{kx}$ and $|\langle B \rangle| = C_{13}^{kx}$. Finally, pulling everything together, Eq. (12) becomes

$$C_{12}^{kx} + C_{13}^{kx} \leq \sqrt{1 + \sqrt{1 + 8 \cos \theta}}. \quad (14)$$

To test the quality of this bound, we plot it in Fig. 2 along with our numerical findings. The above bound turns out to be good, as can be clearly seen in Fig. 2.

Although the mean of the frequency distribution is independent of θ , the reduction in maximal value is due to the lowering of the standard deviation of the distribution induced by increasing incompatibility. The behavior obtained above remains qualitatively similar for any two noncommuting operators, say $C_{12}^{k_1 k_2}$ and $C_{13}^{l_1 l_2}$ in the sum while the maximal value remains same for two commuting operators in $\sum_{i=2}^N C_{1i}^{\alpha\beta}$. For example, we find that the maximum of $C_{12}^{kx} + C_{13}^{kx}$ matches with that of $C_{12}^{xx} + C_{13}^{xx}$ since C_{12}^{kx} commutes with C_{13}^{xx} . This further reinforces the conclusion that the reduction of the maximal value is due to the incompatibility of operators. Such a reduction of maximal values for incompatible operators is observed for higher N values as well.

B. Equivalent shareability rule for classical part of discord and local work

We now concentrate our analysis on the classical part of QD and local work. As we have argued, the classical correlators have a completely different origin than the CQD and LW and hence we may expect some qualitative differences between classical correlators and CQD or LW with the increase of N . Finally, we also compare the trends of f obtained for CQD and LW.

The statistical analysis leads to the emergence of some important features which we now list below:

(1) *f distribution*. The shape of the frequency distribution of $\sum_{i=2}^N C_{1i}^D$ and $\sum_{i=2}^N C_{1i}^{LW}$ for $N \leq 6$ is similar to that obtained from classical correlators, as seen by comparing Figs. 1 and 3.

(2) *Mean from CQD and LW*. Unlike the classical correlators, for which the mean of the f distribution remains almost invariant upon changing N , the mean of the f distribution for the CQD and LW decreases monotonically upon increasing N (compare Tables II and III). Surprisingly, we find that means of the distribution obtained from CQD and LW behave even quantitatively similarly.

(3) *Standard deviation of the distribution from CQD and LW*. Like the classical correlators, the standard deviation of the distribution decreases progressively upon increasing N .

(4) *Algebraic maxima*. The maximal value of $\sum_{i=2}^N C_{1i}^D$ and $\sum_{i=2}^N C_{1i}^{LW}$ decreases sharply upon increasing N . This prompts us to ask whether we can put an upper bound to the sum for random multiqubit pure states. The question will be addressed in the subsequent sections.

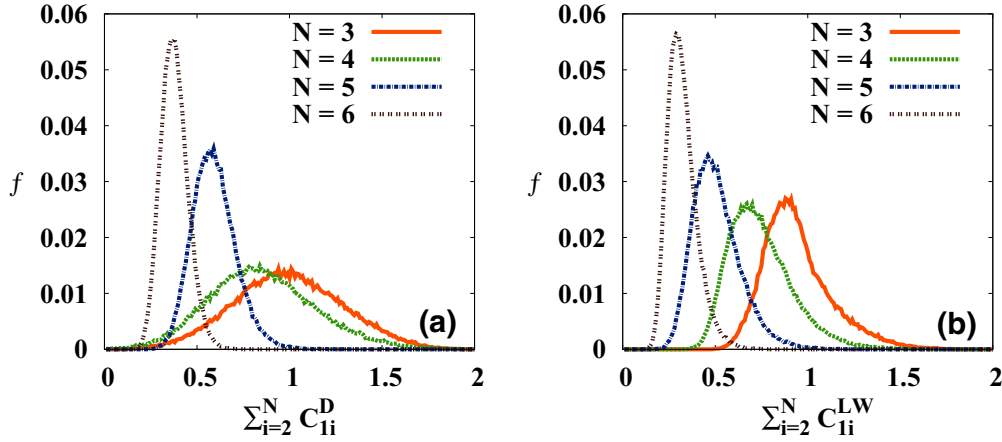


FIG. 3. (a) Frequency distributions of $\sum_i C_{li}^D$, and (b) $\sum_i C_{li}^{LW}$ for $N = 3$ to 6 parties. The other specifications are the same as in Fig. 1.

Interestingly, note that the trends of the frequency distributions for classical correlators are quite different from that of the classical part of quantum discord and local work while the similarities in the distributions are observed for CQD and LW even when they are defined from two disjoint notions. It might be worthwhile investigating whether obeying (or disobeying) the postulates of classical correlations has some bearing on the differences or similarities in the observed features.

C. Features for other measures of classical correlation

Apart from the CC measures discussed above, we also consider two other measures of CC. The first one is just the squares of the classical correlators, $(C^{kl})^2$, instead of taking their absolute values to ensure their non-negativity. Taking it as a measure of CC, we find that it possesses qualitatively similar features as obtained by using the absolute values. However, in this case, the frequency distribution is highly skewed to the left (see Fig. 4), especially for a small number of parties. This is due to the fact that squaring has actually made the correlation values smaller since they are already (typically) less than unity. It also explains why the mean values of the frequency distribution are smaller compared with the case with absolute values of the correlations. When the absolute values are considered, it does not suffer from unnecessary value reduction, and hence supports our choice of considering absolute values to scale the values of the quantity from 0 to 1.

The second one is the maximal mutual information between local measurement results performed on a two-party

state ρ , and is defined as follows:

$$C^I = \max_{\Pi_a, \Pi_b} I(\Pi_a \otimes \Pi_b \rho), \quad (15)$$

where $I(AB) = H(A) + H(B) - H(AB)$ denotes the mutual information content of the measurement statistics, with $H(\cdot) = -\sum_i p_i \log_2 p_i$ being the Shannon entropy. We now compute the frequency distribution of $\sum_{i=2}^N C_{li}^I$ and, by comparing Figs. 1 and 5, find the statistical properties to be almost identical to those obtained by other CCCs.

IV. DISTRIBUTIONS OF CLASSICAL CORRELATIONS FOR CONSTRAINED RANDOM STATES

Let us now move to the investigations of the shareability of classical correlations for randomly generated multipartite states when a fixed amount of a particular physical property that can be both classical or quantum is available. Moreover, we examine how the maximal values of the CC measures can depend on the constraints, i.e., the choice and the range of the physical quantity of the random states. Like before, we perform our analysis for $3 \leq N \leq 6$.

A. Conventional classical correlators under constraints

We now impose constraints either by fixing the range of the sum of bipartite CCC in transverse direction or by fixing the content of the genuine multipartite entanglement [51,55] of the randomly generated states. The latter can also answer the role of classical correlators on a multipartite entanglement measure.

TABLE III. Mean and standard deviation of f for $\sum_i C_{li}^{LW}$ and the maximum of it are tabulated. For other specifications, see Table II.

TABLE II. Mean and standard deviation of the frequency distribution are obtained for $\sum_i C_{li}^D$ with different values of $N \leq 6$. The maximum of the sum is also computed by increasing N . The other specifications are same as in Table I with the exception that the number of states sampled for each N is 10^5 .

	N			
	3	4	5	6
Mean	0.989	0.848	0.587	0.373
Sd	0.291	0.289	0.117	0.073
Max val	1.946	2.207	1.337	0.925

	N			
	3	4	5	6
Mean	0.937	0.741	0.503	0.316
Sd	0.183	0.172	0.128	0.079
Max val	1.877	1.962	1.380	0.883

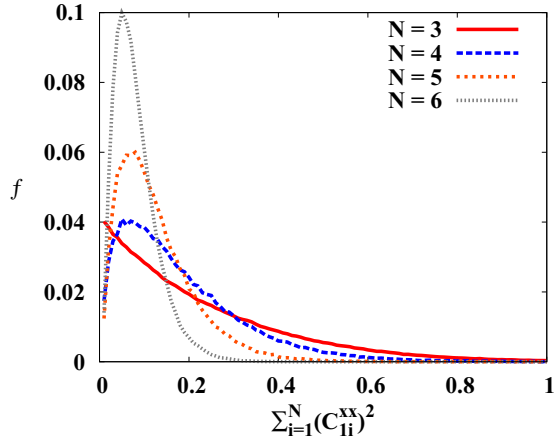


FIG. 4. Frequency distribution of $\sum_{i=1}^N (C_{1i}^{xx})^2$. The fraction f of states (vertical axis) is plotted against $\sum_{i=1}^N (C_{1i}^{xx})^2$ (horizontal axis) with a bin size of 0.01. Total number of random states generated for the analysis for each N is 10^5 . All the axes are dimensionless.

Fixed ranges of CCC. Let us first reveal how restrictions on classical correlators in a fixed direction effect the distribution of correlators in the transverse direction for multiqubit random states. Without loss of generality, we choose to study the distribution of C^{yy} for a fixed values of C^{xx} . In particular, we consider how the average and maximum value of $\sum_{i=2}^N C_{1i}^{yy}$ depends on a given amount of $\sum_{i=2}^N C_{1i}^{xx}$ possessed by the random pure states. We lay out our findings below:

(1) *Three-party states.* For $N = 3$, we find that both the maximum and average of $C_{12}^{yy} + C_{13}^{yy}$ decreases with the increase of a quantity, $C_{12}^{xx} + C_{13}^{xx}$, see Fig. 6(a). It suggests that sum of bipartite classical correlators in transverse directions play a complementary role as confirmed by the behavior of both average and maximal values. A similar feature is observed for $N = 4$. It is important to note that such a dual behavior can also be seen if we choose any two noncommuting classical correlators. This feature can be also viewed as a consequence of ‘‘correlation complementarity’’ as analyzed in Sec. III A 1.

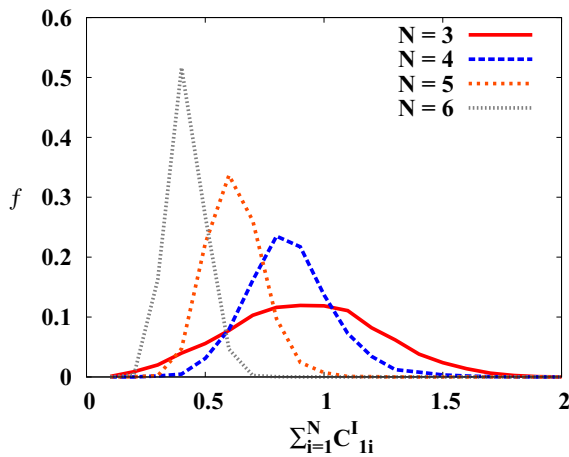


FIG. 5. Frequency distribution (f) of $\sum_{i=2}^N C_{1i}^I$ (vertical axis) vs $\sum_{i=2}^N C_{1i}^I$ (horizontal axis) as defined in Eq. (15). All other specifications are same as in Fig. 4.

(2) *Higher number of parties.* On the contrary, a qualitatively different behavior is observed when $N \geq 5$; specifically, we observe that when the sum of the bipartite correlators in a particular direction grows, the average of the sum of bipartite correlators in the transverse direction remains almost constant, see Figs. 6(c) and 6(d). Note that the maximal value of $\sum_i C_{1i}^{yy}$ also shows an initial increase with the increase of $\sum_i C_{1i}^{xx}$ but then displays the opposite behavior.

The above results reveal that, unlike the unconstrained case, the features of these classical correlators in this constrained scenario strongly depend on the number of qubits of the sampled random states. For $N = 3$, when the maximal value is close to the algebraic maximum, we get a strong ‘‘complementarity-type’’ behavior while a completely different picture emerges with higher values of N . Such an absence of complementarity relation between CCCs in transverse directions for random states can be a consequence of the fact that the gap between the allowed maximal value of $\sum_i C_{1i}^{kk}$ and the algebraic maximum value for random states increases with N and at the same time, the standard deviation decreases (see Table I).

Fixed ranges of GGM. Let us now consider the random states which are segregated based on their genuine multiparty entanglement content (as measured by generalized geometric measure [51,56]). Specifically, we compute $\sum_i C_{1i}^{xx}$ for all the random states having GGM values between say, α and β , where α and β are fixed by the bin values, i.e., $\beta - \alpha = 0.01$ in our case and finally, we compute the average as well as the maximum of $\sum_i C_{1i}^{xx}$. Note here that, among Haar uniformly generated states, the mean of GGM goes towards its maximum value with the increase of number of parties [38–41]. It implies that the bipartite content of entanglement decreases with N . On the other hand, the observations for the distributions of bipartite classical correlators in random multipartite states are as follows (see Fig. 7):

(1) We find that the average value of $\sum_i C_{1i}^{xx}$ is almost independent of the GGM content of sampled random states. In this respect, notice that the average value remains almost constant also for the unconstrained case, see Table I. The feature of the constancy of the average value is independent of the number of qubits, N . It is also important to stress that, although the mean of multipartite entanglement increases with N , and hence $\sum_i E(\rho_{1i})$ decreases, with E being any entanglement measure, the effects of such behavior cannot be captured only by $\sum_i C_{1i}^{xx}$.

(2) Unlike the average values, the maximal value of $\sum_i C_{1i}^{xx}$ for a fixed GGM does not follow any strict pattern. However, it also does not change considerably with the GGM values of the sampled random states.

We will contrast this behavior with that obtained for the other CC measures considered in this paper in subsequent sections.

B. Classical part of quantum discord and local work for a fixed quantum correlation

Classical discord for a fixed content of local work. Let us fix the sum of the amount of local work from various bipartite cuts of a multiparty state, i.e., when the value $\sum_{i=2}^N C_{1i}^{LW}$ lies

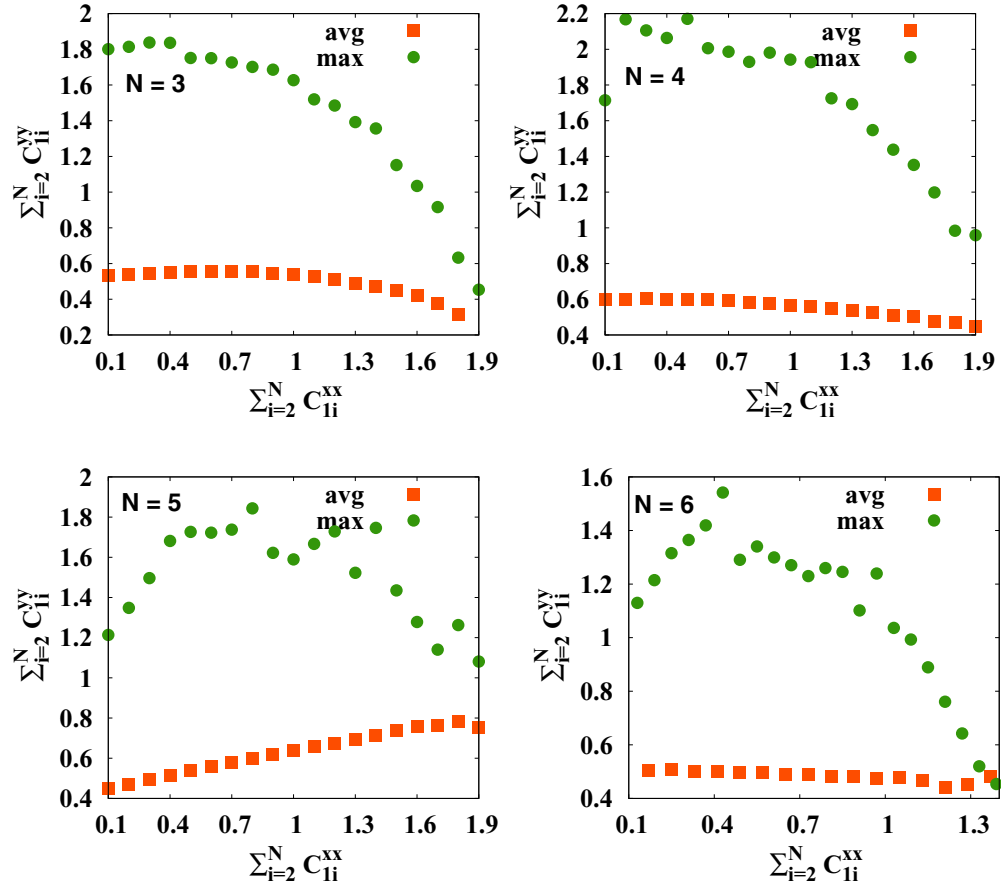


FIG. 6. Average (avg) and maximum values (max) of $\sum_{i=2}^N C_{1i}^{yy}$ (ordinate) for random N -party states possessing a definite amount of $\sum_{i=2}^N C_{1i}^{xx}$ (abscissa). Squares represent the average values while circles are for the maximum value. $N = 3$ and 4 are in the upper panel while in the lower panel from left, $N = 5$ and 6 are displayed. Here the bin size is set to 0.1 . All axes are dimensionless.

between α and β with $\beta - \alpha$ being taken as 0.01 , we find the average and the maximal value of $\sum_{i=2}^N C_{1i}^D$.

Our analysis reveals an emergence of a universal feature independent of the total number of qubits, N .

(1) *Average of CQD with LW constraints.* For a fixed amount of $\sum_{i=2}^N C_{1i}^{LW}$, we observe that the average of $\sum_{i=2}^N C_{1i}^D$ remains almost constant for high N . The change in average can only be seen with $N = 3$, as shown in Fig. 8.

(2) *Maximum under constraints.* The pattern of $\max \sum_{i=2}^N C_{1i}^D$ with respect to $\sum_{i=2}^N C_{1i}^{LW}$ is more drastic as compared with the average of the distribution. The pattern can be divided into two parts—for low values of $\sum_{i=2}^N C_{1i}^{LW}$ ($\lesssim 1$), $\max \sum_{i=2}^N C_{1i}^D$ increases with the increase of $\sum_{i=2}^N C_{1i}^{LW}$ while, interestingly, a complementarity-type relation emerges when $\sum_{i=2}^N C_{1i}^{LW} \gtrsim 1$. Specifically, in a latter case, we get a decrease in $\max \sum_{i=2}^N C_{1i}^D$ values which ultimately become vanishingly small when the sum of local works goes close to its maximal values, see Fig. 8. Such a behavior can also be understood from the examples illustrated in Sec. II A and when $\max \sum_{i=2}^N C_{1i}^D$ and $\max \sum_{i=2}^N C_{1i}^{LW}$ are studied for a given value of multipartite entanglement.

Fixed multipartite entanglement reveals dual nature of CQD and LW. For a given amount of GGM in random three-, four-, five-, and six-qubit states, we observe a dual pattern in the maximum values for bipartite distributions of

classical discord and local work, especially for $N = 3$ [comparing Figs. 9(a) and 9(d)]. In particular, the maximal values of $\sum_{i=2}^N C_{1i}^D$ increase monotonically with increasing values of GGM, while we get the opposite feature for $\sum_{i=2}^N C_{1i}^{LW}$. Maximum of $\sum C_{1i}^{LW}$ always decreases with the increase of GGM. Let us now move to the average values of $\sum_i C_{1i}^{LW}$ and $\sum_i C_{1i}^D$ with GGM. For $N \geq 4$, $\sum_i C_{1i}^{LW}$ always decreases while $\sum_i C_{1i}^D$ remains almost constant to a low value with the increase of GGM. As mentioned earlier for random states, it is known that mean GGM increases with N and therefore one may expect low bipartite entanglement with increasing N . We find that $\sum_i C_{1i}^D$ and $\sum_i C_{1i}^{LW}$ also follows the same trend as one may expect for bipartite entanglement. Moreover, comparing Figs. 7 and 9, it can again be established that the distributions of CCC among subsystems of random multipartite states are quite distinct compared with that of the CQD and LW.

Remark. The properties when the constrained case is reanalyzed using C^I (maximal mutual information between local measurement results) remains almost identical to the statistical features obtained for the CCCs.

V. BOUNDING CLASSICAL CORRELATIONS

As shown in Sec. II A, there always exists a quantum state for which the sum of bipartite classical correlations $\sum_{i=2}^N C_{1i}$

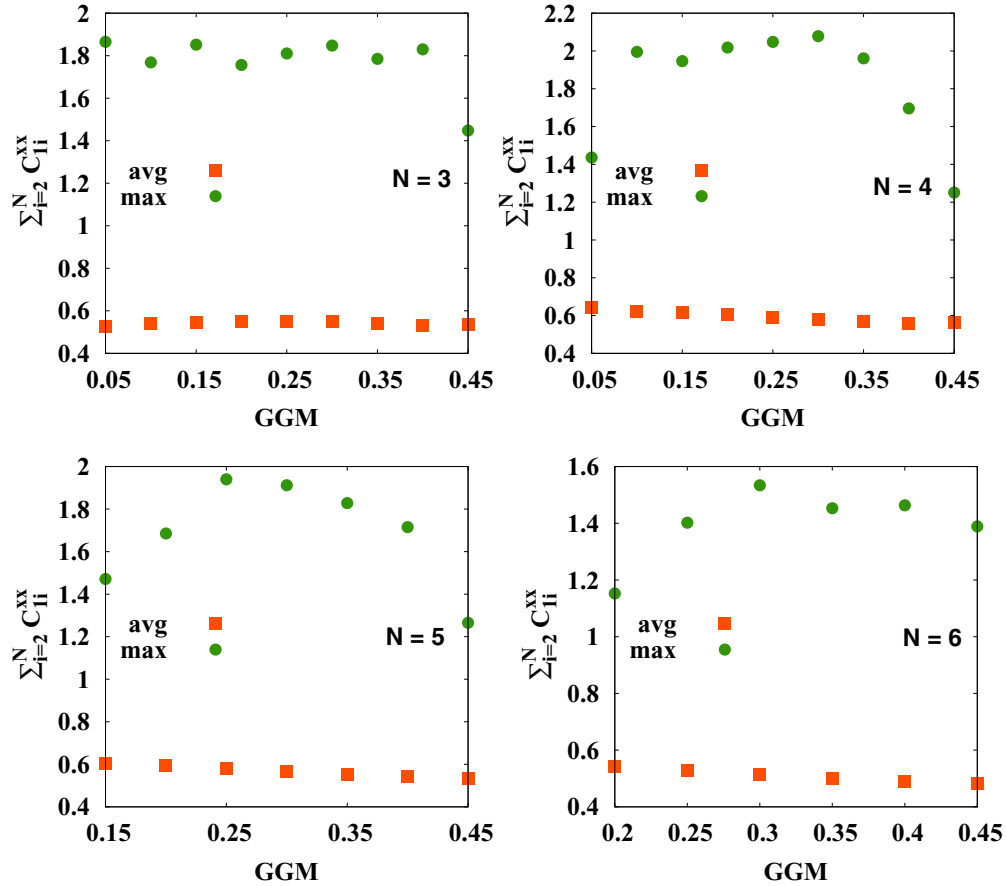


FIG. 7. Plot of an average and maximum of $\sum_{i=2}^N C_{ii}^{yy}$ (y axis) for random states having a fixed genuine multiparty entanglement content as measured by GGM (x axis). Other specifications are same as in Fig. 6, with the exception that the bin size in this case is 0.05. All axes are dimensionless.

reaches the sum of the maximum of individual classical correlations. However, the results obtained in Secs. III and IV for Haar uniformly generated states strongly suggest that the measure-zero subset of states possibly possesses the algebraic maximum value and therefore, for almost all states of the state space, $\sum_{i=2}^N C_{ii}$ can be bounded by a smaller value than the algebraic maximum. Moreover, we observe that, with increase in the number of parties, maximal values for all the classical correlation measures decrease and the gap between the algebraic maxima and the maxima for random states increases.

Here we want to focus again on the upper bound of CC measures, motivated from the concept of monogamy of quantum correlations. It is clear from the examples presented in Sec. II A that CCs, in general, do not satisfy monogamy relation, thereby making it different from QC measure. However, we intend to take a much more closer look at it for random states, since the results indicate that, for high values of N , the upper bound, $C_{1:\text{rest}}$, on the shareability of CC measure, may not be a bad bound for randomly generated quantum states. In particular, we construct a score for classical correlations as well, purely via a formal analogy, examine the distribution of monogamy scores for any classical correlation measure C given by $\delta_C = C_{1:\text{rest}} - \sum_{i=2}^N C_{ii}$ and track the percentage of random states that do not satisfy the constructed monogamy relation.

A. Monogamy-based upper bound for classical correlators

As the prototypical classical correlator, we take C^{zz} . First, note that, for $C_{1:\text{rest}}^{zz}$, the “rest” defines an $N - 1$ qubit state formed by the parties, $2, 3, \dots, N$. Therefore, the second z in the superscript of $C_{1:\text{rest}}^{zz}$ represents the spin- z operator for the 2^{N-1} dimensional system which in turn corresponds to a spin of $s = \frac{2^{N-1}-1}{2}$. For spin s , the magnetization along the z direction is measured by $\Lambda^z(s)$, whose matrix elements in the computational basis are given by

$$[\Lambda^z(s)]_{ij} = 2(s - i)\delta_{ij} = 2(s - j)\delta_{ij}, \tag{16}$$

where $0 \leq i, j \leq 2s$. It defines a diagonal matrix with entries $\text{diag} \{2s, 2s - 2, 2s - 4, \dots, -2s + 2, -2s\}$. Note that the maximal value of $\Lambda^z(s)$ is $2s$. Thus, we scale and define

$$C_{1:\text{rest}}^{zz} = \frac{1}{2s} |\text{tr}(\rho_{12\dots N} \sigma_1^z \otimes \Lambda_{23\dots N}^z(s))|. \tag{17}$$

Having laid out the tools, we now compute the monogamy score for $\delta_{C^{zz}} = C_{1:\text{rest}}^{zz} - \sum_{i=2}^N C_{ii}^{zz}$ for $N = 3, 4, 5$, and 6 . Our investigations from the frequency distribution of $\delta_{C^{zz}}$ reveal that all randomly generated states are nonmonogamous, irrespective of the values of N . Moreover, with increasing N , the f distribution of monogamy scores also does not change much and, as mentioned, all the randomly generated state remain nonmonogamous, i.e., ubiquitously follow a polygamy

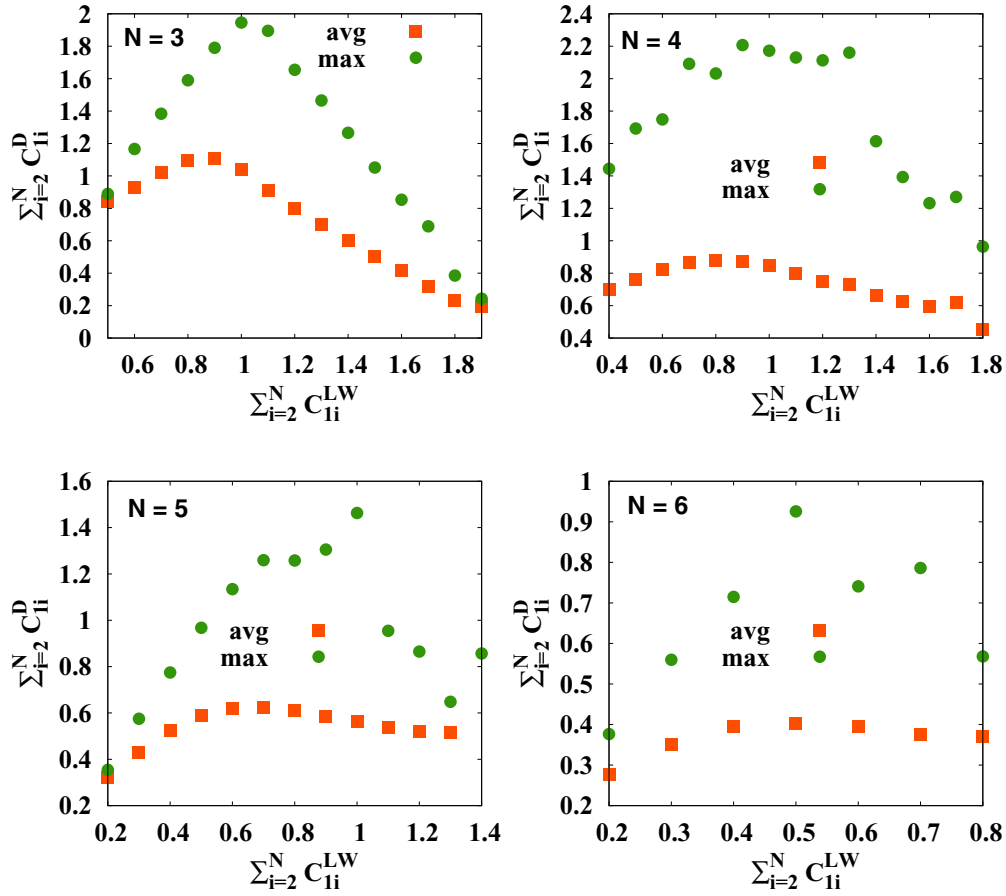


FIG. 8. For a given amount of $\sum_{i=2}^N C_{li}^{LW}$ (horizontal axis), average and maximal values of $\sum_{i=2}^N C_{li}^D$ (vertical axis) for random states is plotted for different values of $N \leq 6$. For other specifications, see Fig. 6.

relation. Furthermore, note that our conjectured $\Lambda^z(s)$ cannot be written as a sum of local magnetizations $\oplus_{i=2}^N \sigma_i^z$. This suggests that our proposed bound, as inspired from monogamy,

is not a particularly good one in this case, as also depicted in Fig. 10. We will contrast the results with classical discord and local work in the subsequent section.

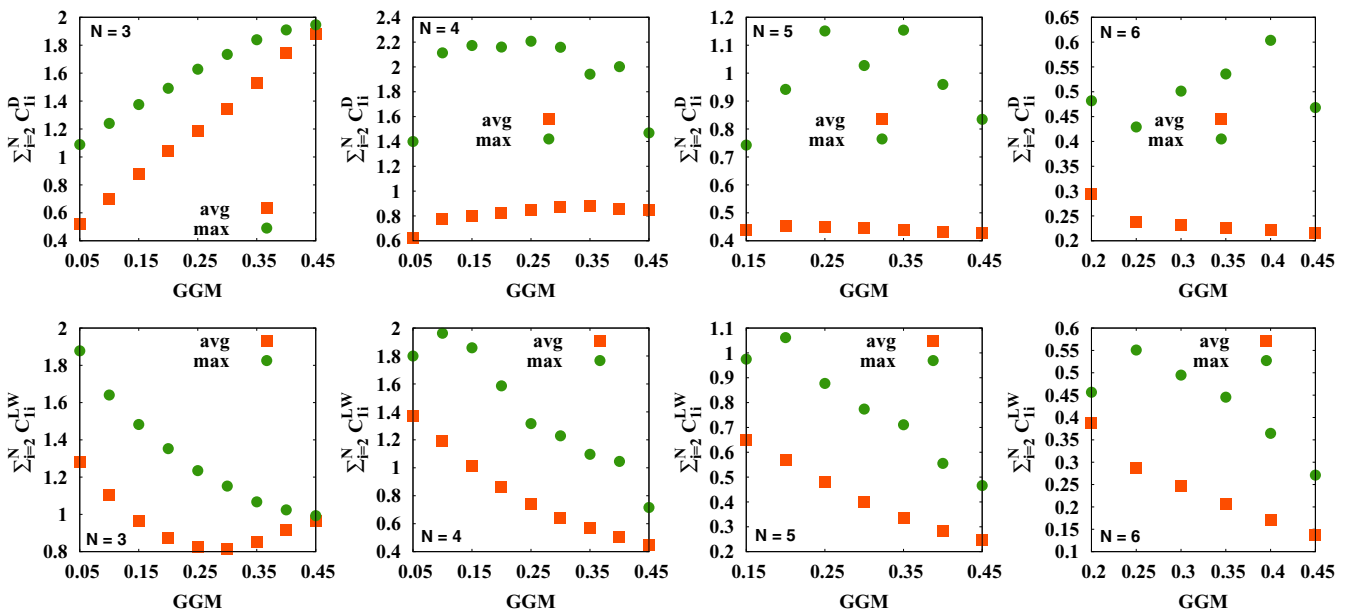


FIG. 9. Upper panel shows the maximum and average values of $\sum_{i=2}^N C_{li}^D$ (ordinate) vs GGM (abscissa). From left to right, N increases from 3 to 6. Lower panel shows $\sum_{i=2}^N C_{li}^{LW}$ against GGM. Here, the bin size for computation is 0.05. All axes are dimensionless.

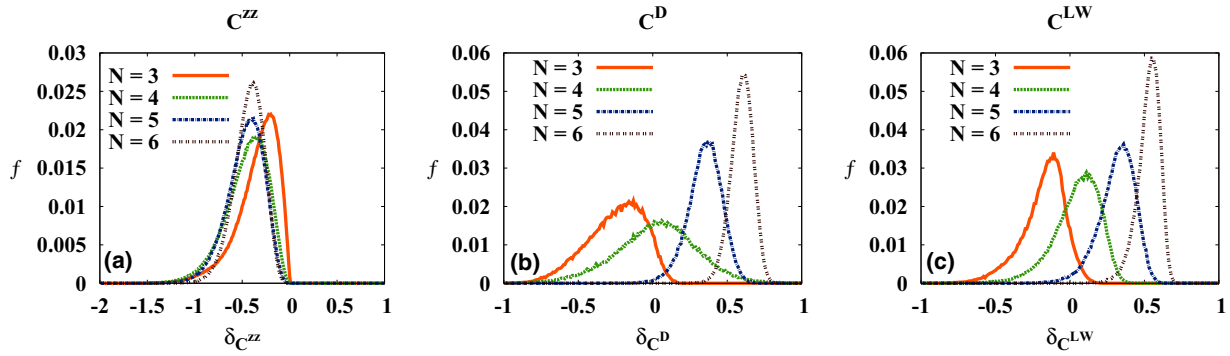


FIG. 10. Monogamy-motivated upper bounds from CC measures. From left to right: the frequency distribution f on the vertical axis is plotted for $\delta_{C^{zz}}$, δ_{C^D} , and $\delta_{C^{LW}}$. N also varies from 3 to 6. All axes are dimensionless.

B. An upper bound for classical part of quantum discord and local work from monogamy

When monogamy-based upper bounds $C_{1:\text{rest}}^D$ and $C_{1:\text{rest}}^{LW}$ on $\sum C_{li}^D$ and $\sum C_{li}^{LW}$ are employed in the case of the classical part of QD and local work, it seems to work much better compared with the case of classical correlators, especially when the random states contain more qubits. The analysis shows yet another point of qualitative difference between the usual classical correlators and the axiomatic classical correlation measures, see Fig. 10.

We track the quality of the bounds by examining the f distribution of the monogamy scores and by computing its statistical parameters of the distribution, see Tables IV and V. In particular, we are interested in the percentage of states that satisfy the monogamy inequality, i.e., the percent of states for which $\delta_{C^D} \geq 0$ and $\delta_{C^{LW}} \geq 0$. Since both classical discord and local work behave almost identically, we list our general observations for both these quantities below:

(1) *Mean and standard deviation of monogamy score.*

Unlike classical correlators, the mean monogamy score progressively shifts from negative to positive values upon increasing N from 3 to 6 while the standard deviation does not follow any strict pattern in these cases (see Fig. 10).

(2) *Percentage of states satisfying monogamy.* For $N = 3$, we find that only a few states satisfy the monogamy relation. However, as N increases to 6, almost all random states ($\approx 99\%$) satisfy the monogamy relation. It suggests that our imposed monogamy-based bound works better when the number of qubits in the generated random states grows. Here it is

TABLE IV. Mean and standard deviation (Sd) of the distribution for the monogamy score of the classical part of discord, δ_{C^D} with a step size of 0.01. \mathcal{M} denotes the percent of monogamous states obtained from randomly generated states. The total number of random states simulated for the analysis for each N is 10^5 .

	N			
	3	4	5	6
Mean	-0.254	0.0172	0.344	0.593
Sd	0.190	0.272	0.113	0.074
\mathcal{M}	6.792	54.606	99.458	100.00

important to note that the monogamy score for QD and WD also increases with N and reaches close to the maximum value with the increase of N [40,57].

(3) *Connecting monogamy-based bound with genuine multipartite entanglement.* Furthermore, if one looks at the data from the f distribution of the classical discord and local work by laying it out on the grids of genuine multipartite entanglement content of the random pure states, we observe an interesting feature. Specifically, when N increases, we know that random states possess more genuine multipartite entanglement on average [38,39]. We observe a strong correlation of the GGM enhancement as N increases, with proclivity of a major percentage of randomly generated states satisfying the monogamy relation for axiomatic CC measures, as depicted in Fig. 11, i.e., high genuine multipartite entangled states satisfy the monogamy of CQD and LW.

VI. CONCLUSION

In a multipartite state, shareability of quantum correlations (QC) among its two-party subsystems is restricted while such a distribution of classical correlations (CC) among parties is not forbidden. In particular, classical correlation content can be maximum simultaneously for all the bipartite reduced density matrices of a multipartite state. It raises a natural question whether all states chosen Haar uniformly from a state space also possess the similar feature. Specifically, our aim was to find out the shape of the distribution for the sum of CC measures obtained from the reduced density matrices of random multipartite states. We also addressed the question of whether the maximum value for shareability of CC is different for random states than that obtained via a class of states.

TABLE V. Similar analysis as in Table IV is performed for the monogamy score of LW, $\delta_{C^{LW}}$.

	N			
	3	4	5	6
Mean	-0.182	0.042	0.310	0.522
Sd	0.145	0.155	0.121	0.075
\mathcal{M}	7.154	65.835	98.264	99.998

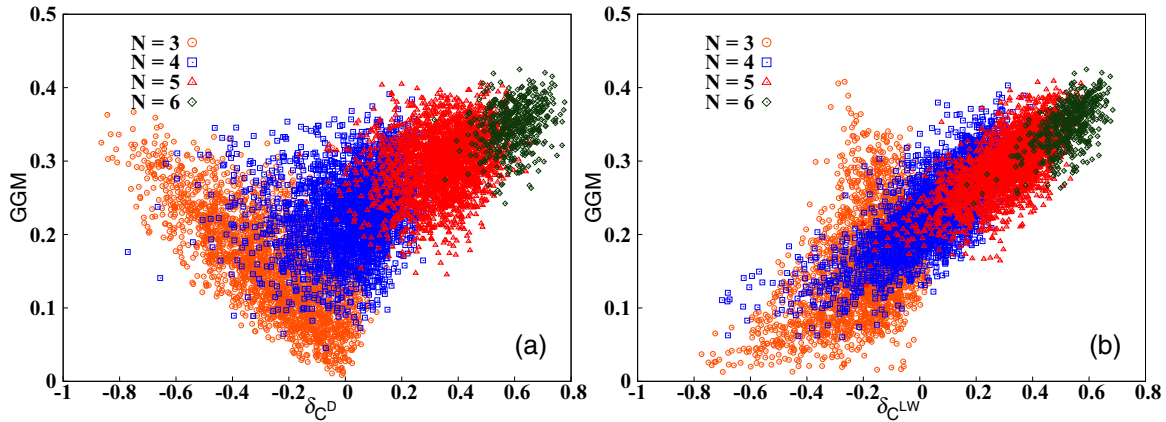


FIG. 11. Scatter plot for comparing δ_{CD} and δ_{CLW} with GGM. We find that, with the increase of N , higher GGM values (ordinate) reveals the monogamous nature of δ_{CD} (abscissa in left panel) and δ_{CLW} (abscissa in right panel). Circles, squares, triangles, and diamonds correspond to $N = 3, 4, 5$, and 6 . All axes are dimensionless.

To investigate it, we considered three kinds of classical correlation measures—conventional classical correlators, CC measure appearing in the definition of quantum discord, and extractable local work in quantum work-deficit. The last two definitions of CC measures obey certain axioms while the first one arises from the measurements performed on two spatially separated systems. Our results showed that, although these axiomatic classical correlation measures have some distinct dissimilarities with classical correlators, the overall behavior of these measures follow a uniform pattern. To study the behavior, we have chosen two directions—we considered the pattern of the distributions obtained for the sum of a given classical correlation measure distributed among two parties of random multipartite states, and we call the situation an unconstrained one. Second, we studied the distribution of classical correlation measures when the states possess a fixed amount of other classical correlation or genuine multipartite entanglement, referred to as the constrained scenario. For our analysis, we generated Haar uniformly random three-, four-, five-, and six-qubit states. In the unconstrained case, we found that their distributions have Bell-like shapes with one long-sided tail, and the mean of the distributions is almost constant for classical correlators with the increase in the number of parties, while the average values of the distribution for the axiomatic CC measures decrease when the number of qubits vary. In the case of classical correlators, we also showed that the noncommutativity in the directions on which classical correlators are defined played an important role in the pattern of shareability of classical correlators.

In the constrained case, we observed that average and maximum values of shareability for conventional classical

correlators does not depend on the genuine multipartite entanglement content although two noncommuting classical correlators depend on each other. Interestingly, we found that, for a given genuine multipartite entanglement, the maximal value of local work and the classical part of quantum discord showed a dual nature in the sense that, when one increases, the other decreases, especially for three-party states.

Counterintuitively, we observed that the maximal value of CC measures, both from the axiomatic and the conventional one, of random multipartite states can be far from the algebraic maximum that CC measures can reach for a certain class of states. Such an observation tempted us to check whether the monogamy-based bound can also be an upper bound for CC measures. We believe that the results obtained here reveal a distinct rule for the distributions of classical correlation measures among subsystems of a global multipartite system. These restrictions are different from the constraints in shareability known for quantum correlation measures.

ACKNOWLEDGMENTS

We acknowledge the support from Interdisciplinary Cyber Physical Systems (ICPS) program of the Department of Science and Technology (DST), India, Grant No. DST/ICPS/QuST/Theme-1/2019/23. Some numerical results have been obtained by using the Quantum Information and Computation library (QIClib). This research was supported in part by the INFOSYS scholarship for senior students. We also thank the anonymous referees for insightful suggestions.

- [1] L. E. Ballentine, *Quantum Mechanics: A Modern Development* (World Scientific Publishing, Singapore, 1998).
 [2] S. Popescu and D. Rohrlich, *Found. Phys.* **24**, 379 (1994).
 [3] W. K. Wootters and W. H. Zurek, *Nature* **299**, 802 (1982); D. Dieks, *Phys. Lett. A* **92**, 271 (1982); R. Jozsa, [arXiv:quant-](https://arxiv.org/abs/quant-ph/0204153)

- [ph/0204153](https://arxiv.org/abs/quant-ph/0204153); A. Lamas-Linares, C. Simon, J. C. Howell, and D. Bouwmeester, *Science* **296**, 712 (2002).
 [4] H. Barnum, C. M. Caves, C. A. Fuchs, R. Jozsa, and B. Schumacher, *Phys. Rev. Lett.* **76**, 2818 (1996); A. Kalev and I. Hen, *ibid.* **100**, 210502 (2008).

- [5] A. K. Pati and S. L. Braunstein, *Nature* **404**, 164 (2000).
- [6] D. Mayers, *Phys. Rev. Lett.* **78**, 3414 (1997); H.-K. Lo and H. F. Chau, *ibid.* **78**, 3410 (1997).
- [7] D. L. Zhou, B. Zeng, and L. You, *Phys. Lett. A* **352**, 41 (2006); A. K. Pati and B. C. Sanders, *ibid.* **359**, 31 (2006).
- [8] K. Modi, A. K. Pati, A. Sen(De), and U. Sen, *Phys. Rev. Lett.* **120**, 230501 (2018).
- [9] V. Coffman, J. Kundu, and W. K. Wootters, *Phys. Rev. A* **61**, 052306 (2000); T. J. Osborne and F. Verstraete, *Phys. Rev. Lett.* **96**, 220503 (2006).
- [10] V. Scarani and N. Gisin, *Phys. Rev. Lett.* **87**, 117901 (2001); *Phys. Rev. A* **65**, 012311 (2001).
- [11] J. Barrett, L. Hardy, and A. Kent, *Phys. Rev. Lett.* **95**, 010503 (2005).
- [12] B. Toner and F. Verstraete, [arXiv:quant-ph/0611001](https://arxiv.org/abs/quant-ph/0611001).
- [13] Ll. Masanes, A. Acin, and N. Gisin, *Phys. Rev. A* **73**, 012112 (2006).
- [14] S. Lee and J. Park, *Phys. Rev. A* **79**, 054309 (2009).
- [15] B. Toner, *Proc. R. Soc. London, Ser. A* **465**, 59 (2009).
- [16] M. Pawłowski and C. Brukner, *Phys. Rev. Lett.* **102**, 030403 (2009).
- [17] J. Oppenheim and S. Wehner, *Science* **330**, 1072 (2010).
- [18] P. Kurzyński, T. Paterek, R. Ramanathan, W. Laskowski, and D. Kaszlikowski, *Phys. Rev. Lett.* **106**, 180402 (2011).
- [19] L. Aolita, R. Gallego, A. Cabello, and A. Acin, *Phys. Rev. Lett.* **108**, 100401 (2012).
- [20] R. Prabhu, A. K. Pati, A. Sen(De), and U. Sen, *Phys. Rev. A* **85**, 040102(R) (2012); G. L. Giorgi, *ibid.* **84**, 054301 (2011).
- [21] R. Prabhu, A. K. Pati, A. Sen (De), and U. Sen, *Phys. Rev. A* **87**, 052319 (2013).
- [22] M.-O. Renou, Y. Wang, S. Boreiri, S. Beigi, N. Gisin, and N. Brunner, *Phys. Rev. Lett.* **123**, 070403 (2019).
- [23] J. S. Kim, G. Gour, and B. C. Sanders, *Contemp. Phys.* **53**, 417 (2012); H. S. Dhar, A. K. Pal, D. Rakshit, A. Sen(De), and U. Sen, in *Lectures on General Quantum Correlations and their Applications*, Quantum Science and Technology (Springer International Publishing, Cham, 2017), pp. 23–64.
- [24] B. M. Terhal, *Lin. Alg. Appl.* **323**, 61 (2001).
- [25] N. Gisin, G. Ribordy, W. Tittel, and H. Zbinden, *Rev. Mod. Phys.* **74**, 145 (2002).
- [26] C. H. Bennett, G. Brassard, C. Crepeau, R. Jozsa, A. Peres, and W. K. Wootters, *Phys. Rev. Lett.* **70**, 1895 (1993).
- [27] M. N. Bera, R. Prabhu, A. Sen(De), and U. Sen, *Phys. Rev. A* **86**, 012319 (2012).
- [28] C. H. Bennett, H. J. Bernstein, S. Popescu, and B. Schumacher, *Phys. Rev. A* **53**, 2046 (1996); M. Koashi and A. Winter, *ibid.* **69**, 022309 (2004); G. Adesso, A. Serafini, and F. Illuminati, *ibid.* **73**, 032345 (2006); T. Hiroshima, G. Adesso, and F. Illuminati, *Phys. Rev. Lett.* **98**, 050503 (2007); M. Hayashi and L. Chen, *Phys. Rev. A* **84**, 012325 (2011); A. Streltsov, G. Adesso, M. Piani, and D. Bruß, *Phys. Rev. Lett.* **109**, 050503 (2012); F. F. Fanchini, M. C. de Oliveira, L. K. Castelano, and M. F. Cornelio, *Phys. Rev. A* **87**, 032317 (2013); Y.-K. Bai, Y.-F. Xu, and Z. D. Wang, *Phys. Rev. Lett.* **113**, 100503 (2014); B. Regula, S. Di Martino, S. Lee, and G. Adesso, *ibid.* **113**, 110501 (2014); M. Enriquez, F. Delgado, and K. Życzkowski, *Entropy* **20**, 745 (2018).
- [29] K. Życzkowski, P. Horodecki, A. Sanpera, and M. Lewenstein, *Phys. Rev. A* **58**, 883 (1998); J. Lee, M. S. Kim, Y. J. Park, and S. Lee, *J. Mod. Opt.* **47**, 2151 (2000); G. Vidal and R. F. Werner, *Phys. Rev. A* **65**, 032314 (2002).
- [30] W. K. Wootters, *Phys. Rev. Lett.* **80**, 2245 (1998).
- [31] M. B. Plenio, *Phys. Rev. Lett.* **95**, 090503 (2005).
- [32] Y.-C. Ou and H. Fan, *Phys. Rev. A* **75**, 062308 (2007); H. He and G. Vidal, *ibid.* **91**, 012339 (2015); J. H. Choi and J. S. Kim, *ibid.* **92**, 042307 (2015).
- [33] W. H. Zurek, *Ann. Phys. Lpz.* **9**, 855 (2000); H. Ollivier and W. H. Zurek, *Phys. Rev. Lett.* **88**, 017901 (2001).
- [34] L. Henderson and V. Vedral, *J. Phys. A: Math. Gen.* **34**, 6899 (2001).
- [35] K. Modi, A. Brodutch, H. Cable, T. Paterek, and V. Vedral, *Rev. Mod. Phys.* **84**, 1655 (2012); A. Bera, T. Das, D. Sadhukhan, S. S. Roy, A. Sen(De), and U. Sen, *Rep. Prog. Phys.* **81**, 024001 (2018).
- [36] Y.-K. Bai, N. Zhang, M.-Y. Ye, and Z. D. Wang, *Phys. Rev. A* **88**, 012123 (2013).
- [37] A. Streltsov and W. H. Zurek, *Phys. Rev. Lett.* **111**, 040401 (2013).
- [38] D. Gross, S. T. Flammia, and J. Eisert, *Phys. Rev. Lett.* **102**, 190501 (2009).
- [39] M. J. Bremner, C. Mora, and A. Winter, *Phys. Rev. Lett.* **102**, 190502 (2009).
- [40] S. Rethinasamy, S. Roy, T. Chanda, A. Sen(De), and U. Sen, *Phys. Rev. A* **99**, 042302 (2019).
- [41] R. Banerjee, A. K. Pal, and A. Sen(De), *Phys. Rev. A* **101**, 042339 (2020).
- [42] J. Oppenheim, M. Horodecki, P. Horodecki, and R. Horodecki, *Phys. Rev. Lett.* **89**, 180402 (2002); M. Horodecki, K. Horodecki, P. Horodecki, R. Horodecki, J. Oppenheim, A. Sen(De), and U. Sen, *ibid.* **90**, 100402 (2003); M. Horodecki, P. Horodecki, R. Horodecki, J. Oppenheim, A. Sen(De), U. Sen, and B. Synak-Radtke, *Phys. Rev. A* **71**, 062307 (2005).
- [43] R. Horodecki, P. Horodecki, and M. Horodecki, *Phys. Lett. A* **200**, 340 (1995).
- [44] N. Brunner, D. Cavalcanti, S. Pironio, V. Scarani, and S. Wehner, *Rev. Mod. Phys.* **86**, 419 (2014).
- [45] S. Sachdev, *Quantum Phase Transitions* (Cambridge University Press, Cambridge, UK, 2009).
- [46] I. Bengtsson and K. Życzkowski, *Geometry of Quantum States: An introduction to Quantum Entanglement* (Cambridge University Press, Cambridge, UK, 2006).
- [47] R. Horodecki, P. Horodecki, M. Horodecki, and K. Horodecki, *Rev. Mod. Phys.* **81**, 865 (2009).
- [48] D. Kaszlikowski, A. Sen(De), U. Sen, V. Vedral, and A. Winter, *Phys. Rev. Lett.* **101**, 070502 (2008).
- [49] C. H. Bennett, A. Grudka, M. Horodecki, P. Horodecki, and R. Horodecki, *Phys. Rev. A* **83**, 012312 (2011).
- [50] D. M. Greenberger, M. A. Horne, and A. Zeilinger, in *Bell's Theorem, Quantum Theory, and Conceptions of the Universe*, edited by M. Kafatos (Kluwer Academic, Dordrecht, The Netherlands, 1989).
- [51] A. Sen(De) and U. Sen, *Phys. Rev. A* **81**, 012308 (2010).
- [52] R. Horodecki, M. Horodecki, and P. Horodecki, *Phys. Lett. A* **222**, 1 (1996).
- [53] G. Tóth and O. Gühne, *Phys. Rev. A* **72**, 022340 (2005).
- [54] S. Wehner and A. Winter, *J. Math. Phys.* **49**, 062105 (2008); *New J. Phys.* **12**, 025009 (2010).
- [55] A. Shimony, *Ann. N. Y. Acad. Sci.* **755**, 675 (1995); H. Barnum and N. Linden, *J. Phys. A* **34**, 6787 (2001); T.-C. Wei and

- P. M. Goldbart, [Phys. Rev. A **68**, 042307 \(2003\)](#); M. Blasone, F. Dell'Anno, S. DeSiena, and F. Illuminati, [ibid. **77**, 062304 \(2008\)](#).
- [56] The generalized geometric measure is a distance-based computable multipartite entanglement measure for pure states which is defined as the distance between a given multipartite pure state and a closest nongenuinely multipartite entangled state. It can be computed if one finds the maximum from the set containing all the maximum eigenvalues obtained from all possible bipartitions of an N -party state $|\psi_{12\dots N}\rangle$.
- [57] A. Kumar, R. Prabhu, A. Sen(De), and U. Sen, [Phys. Rev. A **91**, 012341 \(2015\)](#).